ORGANIC LETTERS

2011
Vol. 13, No. 15
3896–3899

Star-Shaped Pyrrole-Fused Tetrathiafulvalene Oligomers: Synthesis and Redox, Self-Assembling, and Conductive Properties

Masayoshi Takase,* Naofumi Yoshida, Tohru Nishinaga, and Masahiko Iyoda*

Department of Chemistry, Graduate School of Science and Engineering, Tokyo Metropolitan University, Hachioji, Tokyo 192-0397, Japan

mtakase@tmu.ac.jp; iyoda@tmu.ac.jp

Received May 26, 2011

ABSTRACT

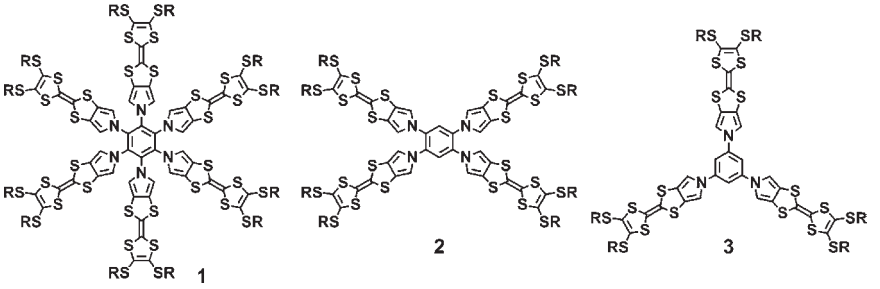

A series of star-shaped pyrrole-fused tetrathiafulvalene (TTF) oligomers 1−3 was synthesized via an S_NAr reaction of fluorinated benzenes with the pyrrolyl sodium salts. Electrochemical and chemical oxidations of 1−3 revealed that a radical cation moiety on each TTF unit was successfully accumulated in all oligomers. Self-assembled structures of neutral and oxidized species were characterized by SEM and XRD, and their conductive properties of the iodine-doped 1−3 as well as an intermolecular mixed-valence ion radical salt were investigated.

Tetrathiafulvalene (TTF) and its analogues have been intensively studied because of their unique π-donor properties.[1] After the discovery of the high electric conductivity of the charge transfer (CT) complex of TTF and tetracyanoquinodimethane (TCNQ),[2] many TTF analogues have been synthesized from the viewpoint of materials and physical sciences. In general, however, conductive molecular complexes should be studied in a single crystal state, which would be problematic in processing materials for applications. To overcome this problem, a supramolecular system has currently been applied to this area, which facilitates the development of electroactive soft materials. Inspired by Jørgensen and Bechgaad's first example of TTF fibers,[3] other supramolecular structures consisting of TTF derivatives have been constructed by utilizing mainly hydrogen-bonding interactions, together with weaker van der Waals, $\pi-\pi$ stacking, and S···S interactions.[4] Among them, Kato et al. demonstrated that doping of the fibers by iodine vapor resulted in the formation of charge-transfer states exhibiting

(1) For selected reviews, see: (a) Adam, M.; Müllen, K. *Adv. Mater.* **1994**, *6*, 439. (b) Bryce, M. R. *J. Mater. Chem.* **1995**, *5*, 1481. (c) Otsubo, T.; Aso, Y.; Takimiya, K. *Adv. Mater.* **1996**, *8*, 203. (d) Bryce, M. R. *J. Mater. Chem.* **2000**, *10*, 589. (e) Nielsen, M. B.; Lomholt, C.; Becher, J. *Chem. Soc. Rev.* **2000**, *29*, 153. (f) Segura, J. L.; Martín, N. *Angew. Chem., Int. Ed.* **2001**, *40*, 1372. (g) Canevet, D.; Sallé, M.; Zhang, G.; Zhang, D.; Zhu, D. *Chem. Commun.* **2009**, 2245. (h) Hasegawa, M.; Iyoda, M. *Chem. Soc. Rev.* **2010**, *39*, 2420.

(2) Wudl, F.; Smith, G.; Hufnagel, E. *J. Chem. Soc., Chem. Commun.* **1970**, 1453.

(3) Jørgensen, M.; Bechgaard, K. *J. Org. Chem.* **1994**, *59*, 5877.

(4) (a) Kitahara, T.; Shirakawa, M.; Kawano, S.; Beginn, U.; Fujita, N.; Shinkai, S. *J. Am. Chem. Soc.* **2005**, *127*, 14980. (b) Wang, C.; Zhang, D.; Zhu, D. *J. Am. Chem. Soc.* **2005**, *127*, 16372. (c) Kitamura, T.; Nakaso, S.; Mizoshita, N.; Tochigi, Y.; Shimomura, T.; Moriyama, M.; Ito, K.; Kato, T. *J. Am. Chem. Soc.* **2005**, *127*, 14769. (d) Puigmartí-Luis, J.; del Pino, Á. P.; Laukhina, E.; Esquena, J.; Laukhin, V.; Rovira, C.; Vidal-Gancedo, J.; Kanaras, A. G.; Nichols, R. J.; Brust, M.; Amabilino, D. B. *Angew. Chem., Int. Ed.* **2008**, *47*, 1861. (e) Akutagawa, T.; Ohta, T.; Hasegawa, T.; Nakamura, T.; Christensen, C. A.; Becher, J. *Proc. Natl. Acad. Sci. U.S.A.* **2002**, *99*, 5028. (f) Gall, T. L.; Pearson., C.; Bryce, M. R.; Petty, M. C.; Dahlgaad, H.; Becher, J. *Eur. J. Org. Chem.* **2003**, 3562.

(5) (a) Kobayashi, Y.; Hasegawa, M.; Enozawa, H.; Iyoda, M. *Chem. Lett.* **2007**, *36*, 720. (b) Ahn, S.; Kim, Y.; Beak, S.; Ishimoto, S.; Enozawa, H.; Isomura, E.; Hasegawa, M.; Iyoda, M.; Park, Y. *J. Mater. Chem.* **2010**, *20*, 10817. (c) Isomura, E.; Nishinaga, T.; Iyoda, M. *Supramolecular Chem.* **2011**, *23*, 304.

10.1021/ol2014279
Published on Web 07/06/2011

semiconductivity of ca. 10^{-5} S cm^{-1}.[4c] Although other simple TTF derivatives possessing polar functional groups like amide and ester were reported to form gels and fibrous structures with high conductivity upon iodine doping,[5] the synthesis and self-assembly of more sophisticated TTF oligomers with planar cyclic[6] and star-shaped[7] structures have also been reported. In these planar π-systems, a number of TTF units work to enhance cooperative S···S and $\pi-\pi$ interactions and thus make an efficient conduction path through the stacked supramolecular architectures.

With these approaches in mind to make electroactive self-assembled structures, we have designed and synthesized a series of star-shaped pyrrole-fused TTF oligomers **1**–**3**, where TTFs are introduced in a less conjugated manner that still maintains their rigid structures compared with previously reported star-shaped[8a] or dendritic[8b,9] TTF oligomers. On the basis of this molecular design, it is expected that star-shaped structures of TTFs enhance the intermolecular interactions to form one-dimensional columnar assemblies, and less intramolecular conjugation between TTF units contributes to the accumulation of radical cation moiety on TTF oligomers.[9]

Scheme 1. Synthesis of Star-Shaped TTF Oligomers **1**–**3**

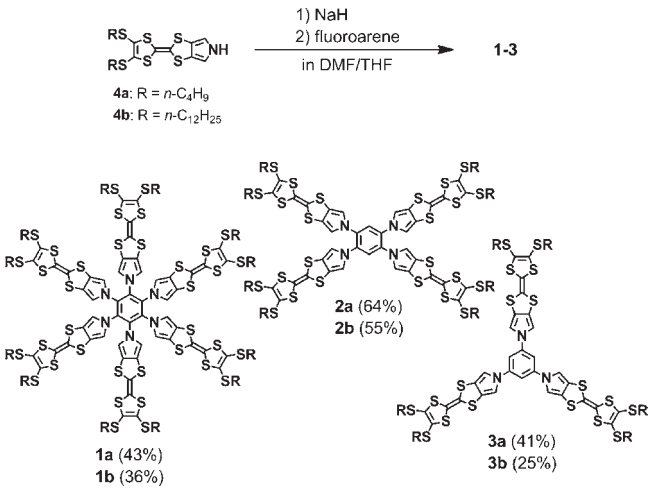

Synthesis of star-shaped TTF oligomers **1**–**3** is based on the nucleophilic aromatic substitution (S_NAr) of fluorinated benzenes (Scheme 1).[10] Pyrrole-fused TTFs **4a**,**b** were chosen as key units[11] because pyrrole–benzene conjugation can be adjustable in terms of torsion angles during assembly and on electrochemical/chemical stimuli. The S_NAr reaction of fluorinated benzenes with the pyrrolyl sodium salts of **4** gave **1**–**3** in moderate yields (25–64%, Scheme 1). Characterization of **1**–**3** was perfomed using ^{1}H NMR, ^{13}C NMR, LDI-TOF MS, and elemental analyses. For example, in the ^{1}H NMR spectra, α-protons of pyrroles were observed at δ 5.93 (**1a**), 6.41 (**2a**), and 6.89 ppm (**3a**), respectively. The signals of **1a** and **2a** at higher fields are ascribable to the ring currents of adjacent pyrrolyl moieties as predicted by theoretical calculations (Figure S7, Supporting Information). Moreover, the exact structure and conformation as well as self-assembly of **3a** were revealed by X-ray single-crystal structure analysis (Figure S6, Supporting Information). Although **3a** forms a dimer in the unit cell, two of the three TTF units are bent simply to fill an empty space, and the other one stacks with a distance of ca. 3.7 Å in contrast to the expected stacked structures with cooperative S···S and $\pi-\pi$ interactions. The torsion angles between the mean planes of the pyrrole and central benzene ring are 11°, 18°, and 31° and 7°, 11°, and 32° for two independent structures, indicating the conformational flexibility of the pyrrole–benzene linkage.

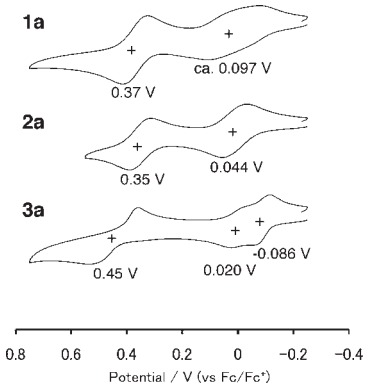

Figure 1. Cyclic voltammograms of **1a**–**3a** (0.1 mM) in benzonitrile with 0.1 M n-Bu_4NPF_6 as the supporting electrolyte, Ag/$AgNO_3$ as the reference electrode, glassy carbon as the working electrode, Pt wire as the counter electrode, and a scan rate of 100 mV/s. Values are half-wave potentials.

The redox behaviors of **1**–**3** were first investigated using cyclic voltammetry (CV) in benzonitrile (0.1 mM) (Figure 1). Although tetrasubstituted **2a** exhibits typical two reversible oxidation waves with half-wave potentials

(6) (a) Enozawa, H.; Hasegawa, M.; Takamatsu, D.; Fukui, K.; Iyoda, M. *Org. Lett.* **2006**, *8*, 1917. (b) Hara, K.; Hasegawa, M.; Kuwatani, Y.; Enozawa, H.; Iyoda, M. *Heterocycles* **2010**, *80*, 909. (c) Anderson, A. S.; Kilsa, K.; Hassenkam, T.; Gisselbrecht, J.-P.; Boudon, C.; Gross, M.; Nielsen, M. B.; Diederich, F. *Chem.—Eur. J.* **2006**, *12*, 8451.

(7) (a) Hasegawa, M.; Takano, J.; Enozawa, H.; Kuwatani, Y.; Iyoda, M. *Tetrahedron Lett.* **2004**, 4109. (b) Hasegawa, M.; Enozawa, H.; Kawabata, Y.; Iyoda, M. *J. Am. Chem. Soc.* **2007**, *129*, 3072.

(8) (a) Christian, C. A.; Bryce, M. R.; Batsanov, A. S.; Becher, J. *Chem. Commun.* **2000**, 331. (b) Christian, C. A.; Goldenberg, L. M.; Bryce, M. R.; Batsanov, A. S.; Becher, J. *Chem. Commun.* **1998**, 509.

(9) For examples of multiple TTF radical cations on oligomeric TTFs, see: (a) Devonport, W.; Bryce, M. R.; Marshallsay, G. J.; Moore, A. J.; Goldenberg, L. M. *J. Mater. Chem.* **1998**, *8*, 1361. (b) Wang, C.; Bryce, M. R.; Batsanov, A. S.; Goldenberg, L. M.; Howard, J. A. K. *J. Mater. Chem.* **1997**, *7*, 1189.

(10) (a) Biemans, H. A. M.; Zhang, C.; Smith, P.; Kooijman, H.; Smeets, W. J. J.; Spek, A. L.; Meijer, E. W. *J. Org. Chem.* **1996**, *61*, 9012. (b) Takase, M.; Enkelmann, V.; Sebastiani, D.; Baumgarten, M.; Müllen, K. *Angew. Chem., Int. Ed.* **2007**, *46*, 5524. (c) Dutta, T.; Woody, K. B.; Watson, M. D. *J. Am. Chem. Soc.* **2008**, *130*, 452.

(11) (a) Jeppesen, J. O.; Takimiya, K.; Jensen, F.; Becher, J. *Org. Lett.* **1999**, *8*, 1291. (b) Jeppesen, J. O.; Takimiya, K.; Jensen, F.; Brimert, T.; Nielsen, K.; Thorup, N.; Becher, J. *J. Org. Chem.* **2000**, *65*, 5794.

(E_{ox}) at 0.044 and 0.35 V (vs Fc/Fc^+), hexasubstituted **1a** and trisubstituted **3a** show broad and split first peaks, respectively, with E_{ox}^1 at ca. 0.097 V (**1a**) and −0.086 and 0.020 V (**3a**), following second peaks with E_{ox}^2 at 0.37 V (**1a**) and 0.45 V (**3a**). Judging from the result of **2a**, which possesses two sets of *ortho*-substituted TTFs, it is suggested that there is no intramolecular charge delocalization between the adjacent TTF units. Therefore, the splitting of the first oxidation waves in **1a** and **3a** is considered to be caused by intermolecular interactions.[12]

To further investigate these phenomena, chemical oxidation of **1a**–**3a** was performed with $Fe(ClO_4)_3$ in a mixture of CH_2Cl_2 and CH_3CN (2:1, v/v). Figure 2 shows the absorption spectral changes of **1a**–**3a** upon the addition of the oxidant. When $Fe(ClO_4)_3$ was added incrementally up to 1 equiv with respect to each TTF unit, the absorption spectra changed dramatically (blue to green spectra in Figure 2). For tetrasubstituted **2a**, the changes were observed with several isosbestic points, indicating that each TTF unit was oxidized from the neutral to the radical cation ($TTF^{\bullet+}$) in a stepwise fashion (Figure 2b). In contrast, for hexa- and trisubstituted **1a** and **3a**, no isosbestic points were observed (Figure 2a,c). For **3a**, a new broad peak around 1850 nm appeared in the presence of 1.5 equiv of the oxidant, which is attributed to the formation of mixed-valence complexes. These results were consistent with the peak splitting of the CV.[7,8,13] On the other hand, the similar appearance of a new peak around the NIR region was not observed for **1a** even at a high concentration. Because such a phenomena was not observed for **2a**, it is concluded that this mixed-valence complex is obtained by an intermolecular fashion, which is completely different from previously reported star-shaped[7,8] and other TTF dimers.[13] From these observations, trisubstituted **3a** appears to form more aggregated structures than other TTF oligomers **1a** and **2a**. In fact, when the temperature of the CH_2Cl_2 and CH_3CN (2:1, v/v) mixed solution of $\mathbf{1a}^{6(\bullet+)}$, $\mathbf{2a}^{4(\bullet+)}$, and $\mathbf{3a}^{3(\bullet+)}$ (0.3 mM) was reduced, inter TTF bonding (π-dimer formation) was induced, which was confirmed by absorption and ESR spectra (Figure S4, Supporting Information). Qualitative order of the intermolecular interactions, $\mathbf{3a}^{3(\bullet+)} \gg \mathbf{1a}^{6(\bullet+)} > \mathbf{2a}^{4(\bullet+)}$, appears to be determined by two factors, i.e., the torsion angles between the pyrrole and central benzene ring and the number of TTF units, and the former would be more effective (the torsion angles estimated by theoretical calculations are 34° (**3**), 45° (**2**), and 59° (**1**), Figure S7, Supporting Information). Again, because tetraradical cation $\mathbf{2}^{4(\bullet+)}$ forms the π-dimer and possibly higher

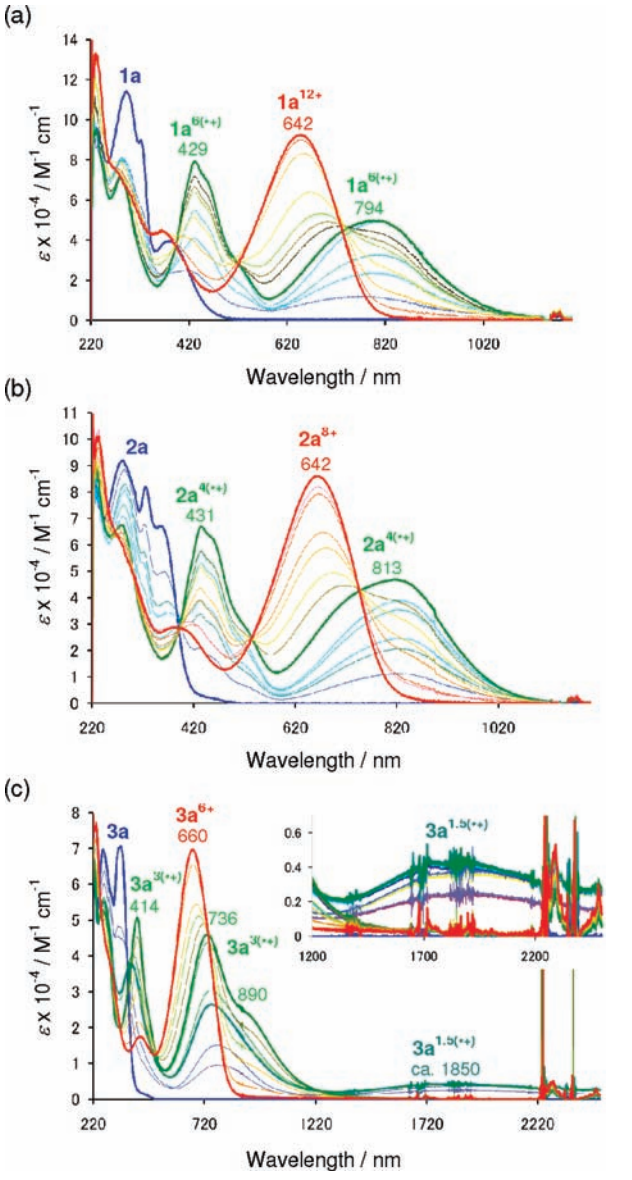

Figure 2. Stepwise oxidation of (a) **1a** (0.03 mM), (b) **2a** (0.05 mM), and (c) **3a** (0.02 mM) with incremental addition of $Fe(ClO_4)_3$ in a mixture of CH_2Cl_2 and CH_3CN (2:1, v/v) at room temperature. The blue line indicates the neutral absorption spectra, the green line the multiple TTF radical cations $\mathbf{1a}^{6(\bullet+)}$–$\mathbf{3a}^{3(\bullet+)}$, and the red line the TTF dications $\mathbf{1a}^{12+}$–$\mathbf{3a}^{6+}$.

aggregates only at low temperatures, the above-mentioned TTF interactions are brought on in an intermolecular fashion, which is preferable for making electroactive supramolecular structures. Further addition of the oxidant to $\mathbf{1a}^{6(\bullet+)}$–$\mathbf{3a}^{3(\bullet+)}$ gave spectral changes with isosbestic points (green to red spectra in Figure 2), which attribute to a decrease of $TTF^{\bullet+}$ and an increase of TTF^{2+}. The above spectral changes were all confirmed by spectroelectrochemical analyses at various applied potentials (Figure S3, Supporting Information).

Once the accumulation of the radical cation moiety on each TTF of **1**–**3** were demonstrated, their self-assembled

(12) One reviewer pointed out the possibility that degenerated molecular orbitals of **1a** and **3a** attributes to the splitting of the redox waves. However, as far as we know, similar phenomena could not be observed in other C_3-symmetrical molecules possessing multiple redox-active components.

(13) (a) Iyoda, M.; Hasegawa, M.; Kuwatani, Y.; Nishikawa, H.; Fukami, K.; Nagase, S.; Yamamoto, G. *Chem. Lett.* **2001**, 1146. (b) Hasegawa, M.; Kobayashi, Y.; Hara, K.; Enozawa, H.; Iyoda, M. *Heterocycles* **2009**, *77*, 837. (c) Nakamura, K-i.; Takashima, T.; Shirahata, T.; Hino, S.; Hasegawa, M.; Mazaki, Y.; Misaki, Y. *Org. Lett.* **2011**, *13*, 3122.

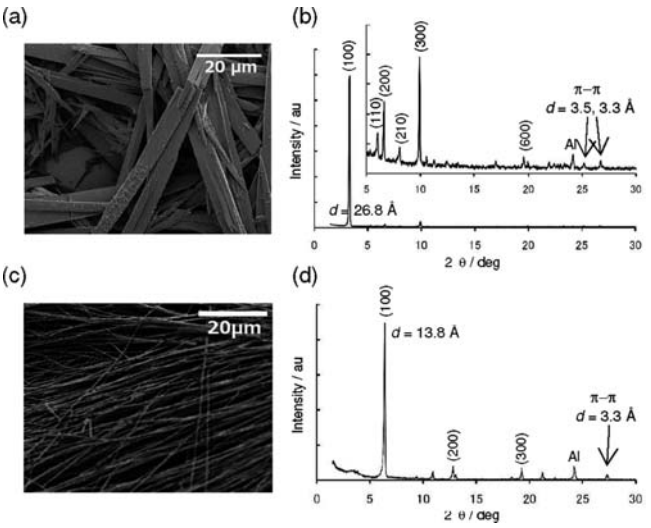

Figure 3. (a) SEM image and (b) XRD profile (2θ = 3.3° (100), 5.7° (110), 6.6° (200), 8.7° (210), 9.9° (300), 19.7° (600), 25.2°, and 26.7°) of **3a-fiber** and (c) SEM image and (d) XRD profile (2θ = 6.4° (100), 12.8° (200), 19.2° (300), and 27.3°) of $\mathbf{3a^{1.5(\bullet+)}\cdot(ClO_4^-)_{1.5}}$**-fiber**.

structures were prepared by mixing an excess amout of poor solvent such as hexane and MeOH to the CH_2Cl_2 and THF solutions, which resulted in the formation of various types of assemblies. When increasing the number of TTF substitutions from trimer (**3a**,**b**) to hexamer (**1a**,**b**) or increasing the length of the alkyl chains from butyl (**1a**–**3a**) to dodecyl (**1b**–**3b**) groups, poor solvents with high polarity are necessary to form assembled structures, resulting in the tendency to form spherical morphologies (Figure S5, Supporting Information). As a representative example, when hexane was added to a CH_2Cl_2 solution of **3a** (0.21 mg/mL in CH_2Cl_2/hexane = 1:4, v/v), a yellow fibrous material was obtained. Scanning electron microscopy (SEM) analysis of **3a-fiber** revealed its micrometer-scale tape structure, whose internal structure was investigated by X-ray diffractometry (XRD) (Figure 3a,b). Thus, a strong (100) and accompanying (110), (200), (210), (300), and (600) reflections are indicative of hexagonal columnar structure (d = 26.8 Å)[14] with additional reflections at 2θ = 25.2° and 26.7° (d = 3.5 Å and 3.3 Å) possibly corresponding to the neutral–neutral and stronger neutral–radical cation (mixed-valence) π–π stackings of TTFs, respectively. Doping of iodine vapor into the compressed pellets of **3a-fiber** produced a black charge transfer complex, which showed an averaged electric conductivity of 1.9×10^{-2} S cm^{-1}.[15] On the other hand, the spin-coat film of **3a**, consisting of a noncrystalline structure as revealed by XRD patterns (Figure S5, Supporting Information), showed a lower conductivity of 2.5×10^{-3} S cm^{-1}. Similar enhancement of the conductivities of the supramolecular structures were also observed for other TTF oligomers **1**–**3** (Table S5, Supporting Information), reflecting the importance of their molecular-level alignments. Interestingly, an averaged conductivity of three single crystals of **3a** after iodine doping was 1.8×10^{-2} S cm^{-1}, which is similar to that of **3a-fiber**, even though their XRD patterns are different (Figure S6, Supporting Information).

Furthermore, not only neutral fibers but also deep green fibrous materials were also formed when a CH_2Cl_2 solution of $\mathbf{3a^{1.5(\bullet+)}\cdot(ClO_4^-)_{1.5}}$ was mixed with an excess amount of hexane (Figure 3c). The XRD pattern of the fibers supports that it is mainly composed of a lamellar structure (d = 13.8 Å)[14] with a π–π stacking distance of d = 3.3 Å (Figure 3d). Thus, an averaged electric conductivity of $\mathbf{3a^{1.5(\bullet+)}\cdot(ClO_4^-)_{1.5}}$**-fiber** was evaluated to be 2.9×10^{-4} S cm^{-1} without further doping,[15] which is a still-rare example of electroactive supramolecular fibers prepared from organic ion radical salts.[7b]

In summary, we have demonstrated the synthesis of a series of star-shaped TTF oligomers **1**–**3** via S_NAr reaction. The less conjugated but still rigid pyrrole–benzene linkages of **1**–**3** gave no intramolecular interactions between neutral, oxidized, and neutral/oxidized TTFs, so that accumulation of redox active TTF units was successful in all star-shaped oligomers. However, possible increment of the charge carrier density brought on by the accumulated radical cation moieties in the oligomers do not seem to contribute effectively to the conductivities of the self-assembled structures. Also, the relationship between the substitution numbers/positions and conductivities of the assembled structures remains to be fully elucidated. Further investigations like a development of well-defined TTF oligomers are currently underway in our group.

Acknowledgment. This work was supported by Grants-in-Aid for Science and Research (Nos. 20850030 and 22245024) from MEXT, Japan, and research grants from The Mazda Foundation and The Kao Foundation for Arts and Sciences. We thank Dr. K. Yamashita (Tokyo Metropolitan University) for help with X-ray crystal structure analysis.

Supporting Information Available. Experimental procedures and the characterization data for all new compounds; Figure S3–S7, Table S5, atomic coordination of the optimized structures of **1**–**3** (B3LYP/6-31G(d)), and X-ray data for **3a** (CIF). This material is available free of charge via the Internet at http://pubs.acs.org.

(14) According to the theoretical calculation, the molecular diameter of **3** (methylthio derivative) is ca. 25 Å and the length of pyrrole-fused TTF unit is ca. 12 Å. See Figure S7 (Supporting Information).

(15) The compressed pellets gave XRD patterns similar to those of the fibrous materials, and the values of conductivities are averages of three runs.